25th ABCM International Congress of Mechanical Engineering
October 20-25, 2019, Uberlândia, MG, Brazil

COB-2019-2192
STUDY OF THE CTE MISMATCH EFFECT IN THE FRACTURE BEHAVIOUR OF COMPOSITE MATERIALS USING LATTICE MODELS

Heloísa Zanardi
Ricardo Afonso Angélico
University of São Paulo, São Carlos School of Engineering, Department of Aeronautical Engineering, São Carlos, Brazil
heloisa.zanardi@usp.br - raa@sc.usp.br

Abstract. *The mismatch of thermomechanical properties between the phases of a composite material can lead to cracks nucleation when this material is submitted to a temperature variation. The prediction of mechanical behaviour via numerical modelling becomes difficult because of the complex crack pattern. One of the strategies that can be used in this context is the lattice models. In these models, the structure can be considered as a network of one-dimensional interconnected elements, and the structural failure can be simulated by the progressive damage of the lattice bars. The composite studied was alumina inclusions surrounded by a glass matrix submitted to a cooling. In this study, a single inclusion was considered, referring to the model proposed by Davidge & Green. The model was applied for two combinations of thermal expansion coefficients. In the first combination, the inclusion thermal expansion is higher than the matrix one; and in the second one, the opposite. The computational tool enables to predict the matrix crack pattern – circumferential and radial cracks for the first and second case, respectively – reported in the literature in both models.*

Keywords: *lattice models, thermomechanical behaviour, properties mismatch, fracture behaviour, heterogeneous materials*

1. INTRODUCTION

One of the most outstanding developments in material science is the advent of composite materials, which combine two or more materials in a single composite. Such combinations allow the attainment of higher specific properties and improve the materials performance when submitted to thermal and/or mechanical loads (Dowling, 2012). Despite of the numerous benefits of composite materials, the assembly of different materials leads to a more complex failure mechanisms, such as the occurrence of cracks coalescence and bifurcation (Talreja, 2014).

Specifically, for the case of a composite material submitted to a temperature variation, the mismatch of the coefficient of thermal expansion (CTE) of each phase can create circumferential, radial or inter-inclusion cracks (Luchini *et al.*, 2016). These cracks can present a complex arrangement that difficult its simulation. One possible simulation approach is the use of lattice models, which represent a continuum domain as a network of bars or beams (van Mier, 1997; Schlangen and van Mier, 1992; Nikolić *et al.*, 2017).

At this context, the present article investigates the mechanical behaviour of a system composed by a single inclusion inserted in a matrix when submitted to a cooling. The crack patterns for different combinations of the thermal expansion coefficients are obtained. The evolution of the overall damage with respect to the temperature variation is investigated.

2. MODEL DESCRIPTION

The composite analysed is presented in Fig. 1. It consist of an alumina cylindrical inclusion of radius r = 0.25 mm surrounded by a glass matrix of radius R = 5 mm. The ratio of 1/20 between the inclusion and matrix radius intends to simulate a infinity medium (as proposed by the Davidge & Green model (Davidge and Green, 1968)). The material properties and denominations were obtained from Tessier-Doyen *et al.* (2006) and are presented in Tab. 1.

The matrix analysed is brittle and its failure is simulated using a damage parameter d, which is defined as:

$$d = \begin{cases} 0 & \varepsilon^* < \bar{\varepsilon} \\ \left(1 - \dfrac{\bar{\varepsilon}}{\varepsilon^*}\right)\left(\dfrac{\gamma}{E_0} - 1\right) & \varepsilon^* \geq \bar{\varepsilon} \end{cases} \tag{1}$$

where E_0 is the undamaged Young modulus, $\bar{\varepsilon}$ is the strain that corresponds to the maximum stress, γ is a parameter

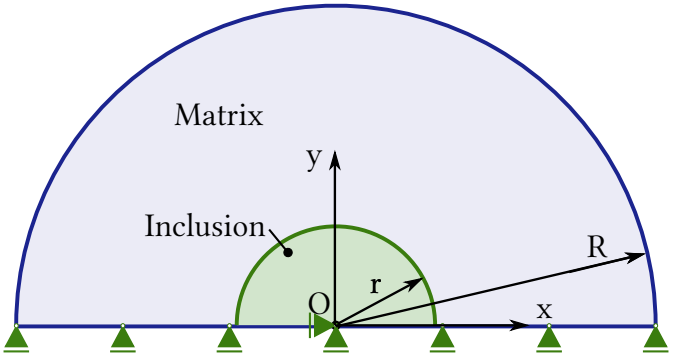

Figure 1. Alumina cylindrical inclusion (r = 0.25) mm surrounded by a glass matrix (R = 5 mm).

Table 1. Material properties extracted from Tessier-Doyen *et al.* (2006).

Material	**Young modulus [GPa]**	**Poisson coefficient**	**CTE*** $[10^{-6}\,^{\circ}C]$
Alumina	340	0.24	7.6
Glass 1 (G1)	68	0.20	4.6
Glass 3 (G3)	72	0.23	11.6

*CTE: Coefficient of Thermal Expansion

related to the damage growth ratio, and ε^* is the maximum strain reached by an element during its loading history. These parameters can be seen in Fig. 2. If the material is unloaded after surpassing $\bar{\varepsilon}$, it will return to the undeformed shape through a curve with a different slope (stiffness). This different slope is called *effective* Young modulus and is given by $E = E_0(1 - d)$.

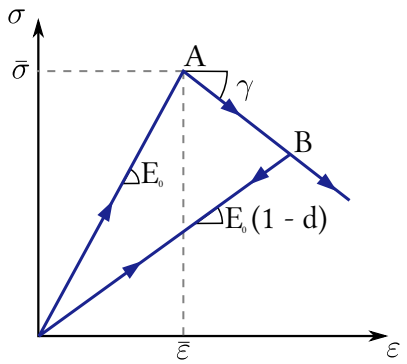

Figure 2. Stress-strain curve for a material axially loaded with the presence of softening and damage.

2.1 NUMERICAL PROCEDURE

The first step of the analysis is the compatibilization between the continuum and discrete (lattice) models through the calibration of the lattice elements stiffness. Such compatibilization is achieved by assuring a kinematic compatibility, i.e., the displacement obtained in both models must be equivalent. In this research, bar elements are used and their stiffness depends on the element length ℓ and cross-section area S.

The response of the continuum model was obtained by a finite element analysis in ABAQUS, where a 10 mm diameter disc submitted to a radial pressure of 10 MPa was simulated. The model was meshed using a non-structured mesh of linear triangular elements (T3) and due to the problem symmetry only a half model was simulated. The bottom of the semicircle is restricted vertically and the centre point is also restricted horizontally.

The lattice model was build using the continuum model mesh, replacing each triangle side by a bar element. An initial stiffness for the bars was imposed, and the model response was obtained using an in-house Finite Element Method (FEM) package. The comparison between the nodal displacements obtained in each model (continuum and lattice) was used to calibrate the bars stiffness.

This procedure was repeated for all three materials presented in Tab. 1 and the values obtained for the *stiffness factor* (ratio between the element cross-section area S and length ℓ) were 0.7039, 0.7313 and 0.7409 for glass 1, glass 3 and

alumina, respectively.

Once the lattice parameters were calibrated, the model is analysed using the finite element package. The nodal displacements are compared to the closed-form solution proposed by Timoshenko and Gere (1961), which is given by:

$$u_r(r) = -p\,r\,\frac{(1-\nu)}{E} \tag{2}$$

In particular for the problem studied herein, the closed-form solution can also be used to calibrate the stiffness factor. However, the problem solution cannot always be written analytically and then a more general calibration procedure using the numerical data have been used in this article.

The results of the radial displacement (in mm) obtained from the analytical and numerical models evaluated in the external radius R = 5 mm are presented in Tab. 2. The error is approximately 3% in both cases. The displacement field for the alumina structure is shown in Fig. 3. The bands are not perfectly circular because of the lattice irregularity.

Table 2. Radial displacements in R = 5 mm for alumina and glasses.

Material	**Analytical**	**Lattice tool**
Alumina	1.117E-4	1.155E-4
Glass G1	5.882E-4	6.078E-4
Glass G3	5.347E-4	5.525E-4

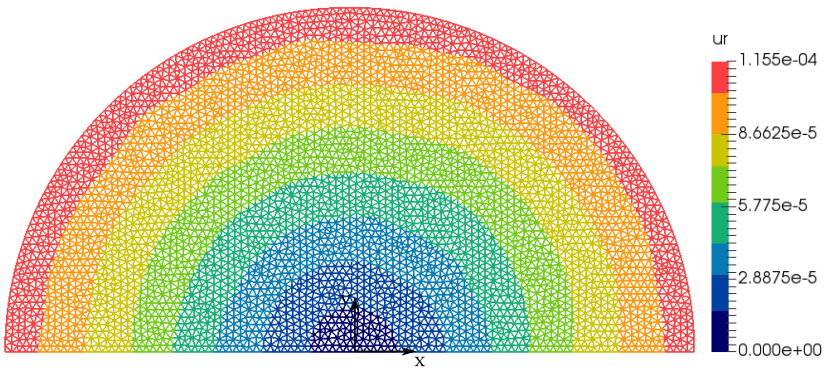

Figure 3. Radial displacement for a alumina disc obtained via lattice model for a uniform radial pressure.

Once a compatible lattice structure was obtained, the damage endured by the material can be simulated by the damage variable d (Eq. (1)). This variable is a function of the strain level and therefore it changes during the loading which introduces a nonlinearity in the problem. Consequently, an iterative procedure is necessary to solve it and, in this research, the procedure adopted was the Newton-Raphson method.

The solution method adopted is the classical FEM formulation which can be found in the literature (Bathe, 2006; Fish and Belytschko, 2007; Zienkiewicz and Taylor, 1977). To introduce the damage variable, it is necessary to consider the effective Young modulus in the formulation, so the element stiffness matrix written in global coordinates gets the form:

$$\mathbf{K}^e = (1-d)\frac{E_0 S}{\ell_e}\begin{bmatrix} \cos^2\theta & \cos\theta\sin\theta & -\cos^2\theta & -\cos\theta\sin\theta \\ & \sin^2\theta & -\cos\theta\sin\theta & -\sin^2\theta \\ sym. & & \cos^2\theta & \cos\theta\sin\theta \\ & & & \sin^2\theta \end{bmatrix} \tag{3}$$

where θ is the angle between the element and the horizontal axis. To take into account the temperature effects (considering a steady-state analysis) the force vector $\boldsymbol{f}$ is:

$$\boldsymbol{f}^e = \begin{Bmatrix} (f_1 - ES\alpha\Delta T)\cos\theta \\ (f_1 - ES\alpha\Delta T)\sin\theta \\ (f_2 + ES\alpha\Delta T)\cos\theta \\ (f_2 + ES\alpha\Delta T)\sin\theta \end{Bmatrix} \tag{4}$$

The global stiffness matrix ($\mathbf{K}^g$) and force vector ($\mathbf{f}^g$) are obtained by the assemblage of the element stiffness matrix and force vector, and it results in a system of the form $\mathbf{K}^g(\mathbf{u})\mathbf{u} = \mathbf{f}^g$, where the nonlinear behaviour can be seen in the dependency of $\mathbf{K}^g$ with $\mathbf{u}$.

2.2 RESULTS

For the model presented previously (Fig. 1), two different combinations of materials were studied: (I) an alumina inclusion surrounded by a glass G1 matrix and (II) an alumina inclusion in a glass G3 matrix. In both models, the composite is cooled down and it is considered that only the matrix withstands damage. The CTE mismatch between the matrix and inclusion can induce cracks in the composite that – according to Tessier-Doyen *et al.* (2006) – are circumferential in the case where the matrix CTE is smaller than the inclusion one (case (I)) and radial for the reciprocal combination (case (II)). Both composites were submitted to a temperature variation of $\Delta T = -500°C$ and evaluated for three different values of the damage law parameter γ: $2\,E_0$, $5\,E_0$ and $10\,E_0$.

The total damage of the model, i.e., the summation of the damages (d) of each lattice bar, was chosen as the parameter of the analysis. Its evolution for each composite simulated is presented in Fig. 4. In Fig. 4(a), the three curves start to grow virtually at the same temperature (close to $250°C$) but they evolve with different slopes, showing a dependency of the total damage with the constant γ. Nevertheless, they all achieve the same level at a temperature T = $325°C$ and for temperatures higher than $350°C$, they increase together. This behaviour mirrors the physical phenomena that happens in the composite interface: the detachment between matrix and inclusion due to the propagation of circumferential cracks. In the second case (Fig. 4(b)), the three curves start to grow from a lower temperature (around $150°C$) and they increase continuously together, showing an independence with γ. Also, the propagation of cracks is not restricted to the interface area, so they propagate throughout the matrix and so the total damage keeps growing.

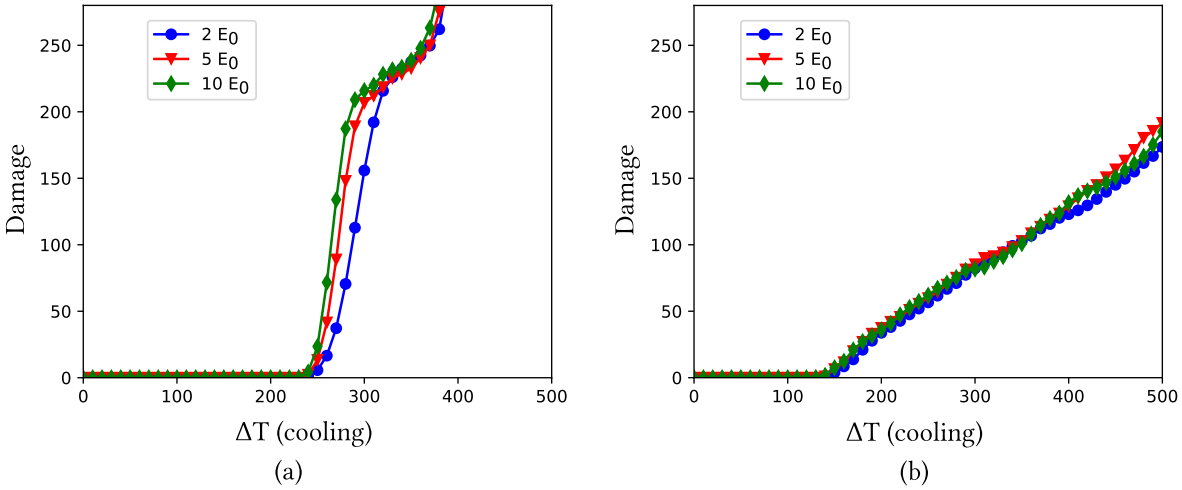

Figure 4. Damage evolution for (a) alumina/glass G1 composite and (b) alumina/glass G3 composite

To allow a better understanding of the crack propagation, a series of snapshots of the analysis were taken. Figure 5 shows the cracks evolution for the first composite (alumina and glass G1) with two different damage parameters ((a) $\gamma = 2\,E_0$ and (b) $\gamma = 10\,E_0$). In both columns the propagation of the circumferential cracks until the complete interface detachment can be seen, but for the first two rows the amount of total damage is higher for the larger γ. In the last row ($T = 380°C$), such difference disappears once the matrix is completely detached from the inclusion. These results are in agreement with the ones presented in Fig. 4(a).

The snapshots for the composite of alumina and glass G3 are presented in Fig. 6. Once again, the comparison is made for two different damage parameters ($\gamma = 2\,E_0$ (a) and $\gamma = 10\,E_0$ (b)). The cracks propagation are very similar in both columns, as it was predicted by the damage curve (Figure 4(b)). For the temperature of $450°C$, it is possible to identify the coalescence between cracks (right-hand side of the image).

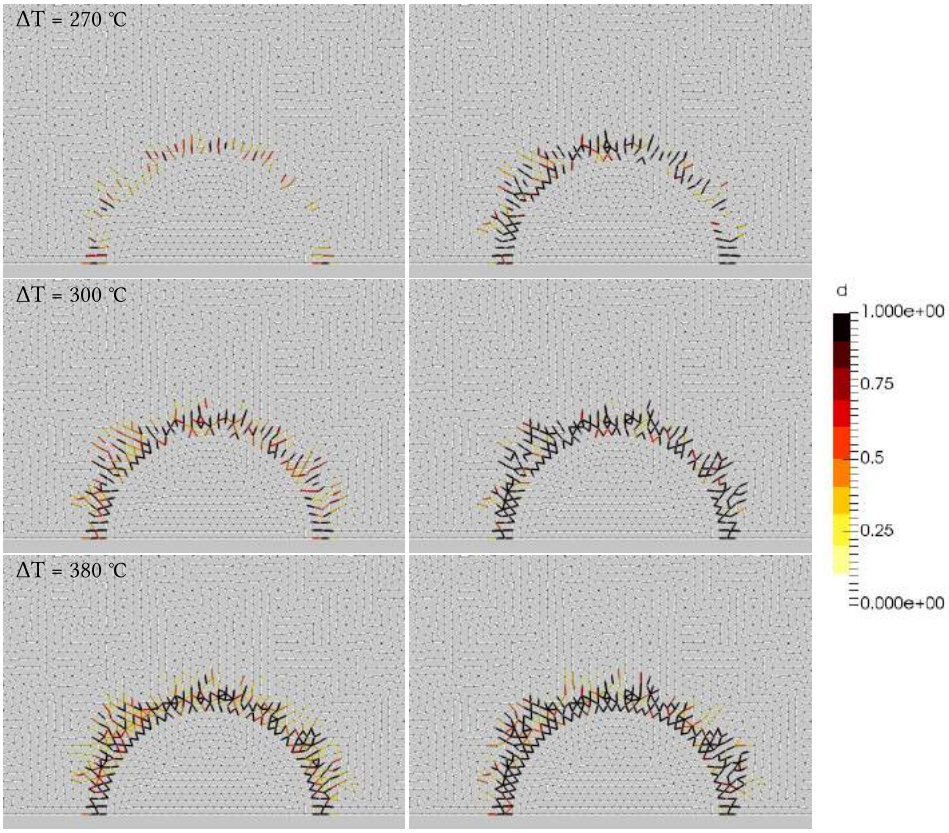

(a) (b)

Figure 5. Snapshots of the circumferential cracks for (a) $\gamma = 2\,E_0$ and (b) $\gamma = 10\,E_0$

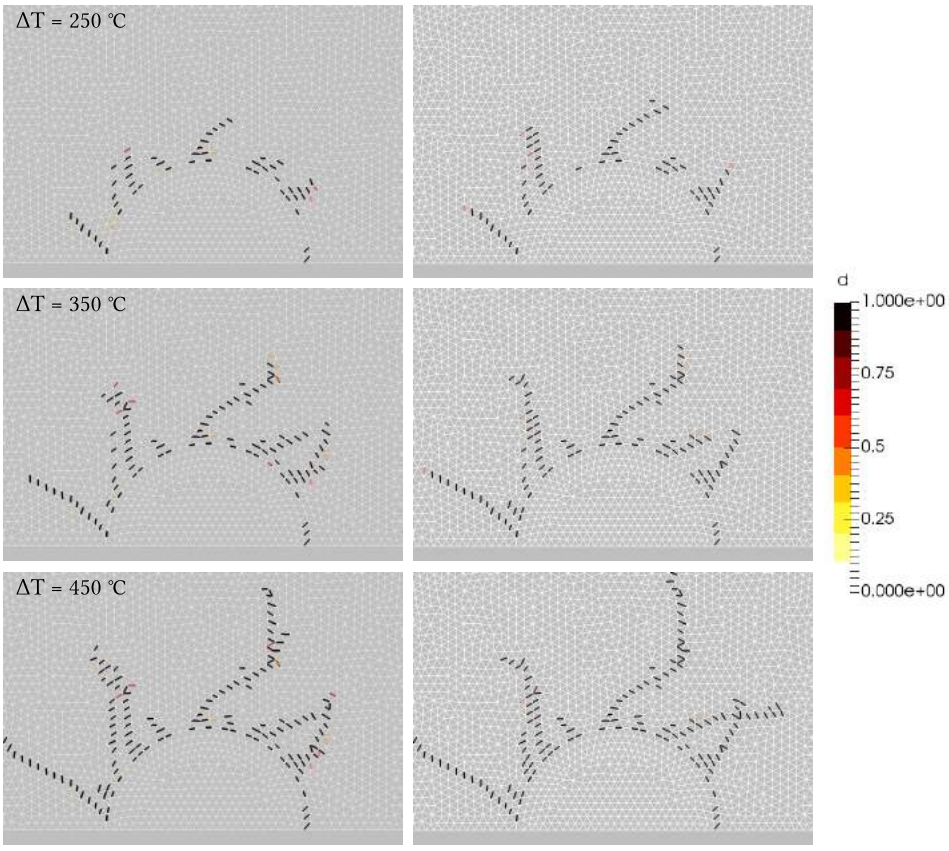

(a) (b)

Figure 6. Snapshots of the radial cracks for (a) $\gamma = 2\,E_0$ and (b) $\gamma = 10\,E_0$

3. CONCLUSIONS

The results of the simulations corroborate the capability of the lattice models to predict the fracture behaviour of composites. In the first composite, where the matrix CTE is smaller than the inclusion one, circumferential cracks were observed and the total damage presented a dependency with the damage parameter. For the second composite, where the matrix CTE is larger than the inclusion one, radial cracks were observed and the total damage showed no dependency with the damage parameter. In both examples, the crack pattern obtained was in agreement with the one foreseen by the literature.

The developed tool can be useful in the simulation of structures submitted to a temperature variation with or without mechanical loads. In particular, it can be used to simulate the mechanical behaviour of composite materials with fragile matrices. The progressive failure of each bar enables to simulate the crack propagation throughout the structure using a simple one-dimensional constitutive law. This approach leads to the possibility of solving complex problems without an excessive computational cost.

4. ACKNOWLEDGEMENTS

The authors would like to thank CAPES for the partial financial support of the present research.

5. REFERENCES

Bathe, K.J., 2006. *Finite element procedures*. Klaus-Jurgen Bathe.

Davidge, R.W. and Green, T.D., 1968. "The Strength of Two-Phase Ceramic/Glass Materials". *Journal of Materials Science*, Vol. 3, pp. 629–634.

Dowling, N.E., 2012. *Mechanical behavior of materials: engineering methods for deformation, fracture, and fatigue*. Pearson.

Fish, J. and Belytschko, T., 2007. "A first course in finite elements".

Luchini, B., Sciuti, V.F., Angélico, R.A., Canto, R.B. and Pandolfelli, V.C., 2016. "Thermal expansion mismatch inter-inclusion cracking in ceramic systems". *Ceramics International*, Vol. 42, No. 10, pp. 12512–12515. doi: 10.1016/j.ceramint.2016.05.013. URL `http://dx.doi.org/10.1016/j.ceramint.2016.05.013`.

Nikolić, M., Karavelić, E., Ibrahimbegovic, A. and Miščević, P., 2017. "Lattice element models and their peculiarities". *Archives of Computational Methods in Engineering*, pp. 1–32.

Schlangen, E. and van Mier, J.G.M., 1992. "Simple lattice model for numerical simulation of fracture of concrete materials and structures". *Materials and Structures*, Vol. 25, No. 9, pp. 534–542. ISSN 00255432. doi:10.1007/BF02472449.

Talreja, R., 2014. "Assessment of the fundamentals of failure theories for composite materials". *Composites Science and Technology*, Vol. 105, pp. 190–201.

Tessier-Doyen, N., Glandus, J. and Huger, M., 2006. "Untypical young's modulus evolution of model refractories at high temperature". *Journal of the European Ceramic Society*, Vol. 26, No. 3, pp. 289–295.

Timoshenko, S.P. and Gere, J.M., 1961. "Theory of elastic stability".

van Mier, J.G., 1997. "Fracture process of concrete: Assessment of material parameters for fracture models". *Boca Rotan FL: CRC Press, Florida*.

Zienkiewicz, O.C. and Taylor, R.L., 1977. *The finite element method*, Vol. 3. McGraw-hill London.

6. RESPONSIBILITY NOTICE

The authors are the only responsible for the printed material included in this paper.